ADVANCED MATERIALS
www.advmat.de

A Streaming Potential/Current-Based Microfluidic Direct Current Generator for Self-Powered Nanosystems

*Rui Zhang, Sihong Wang, Min-Hsin Yeh, Caofeng Pan, Long Lin, Ruomeng Yu, Yan Zhang, Li Zheng, Zongxia Jiao, and Zhong Lin Wang**

Scavenging energy from the ambient environment is a promising approach for independent, sustainable, and wireless operation of self-powered systems.[1] To achieve optimum system performance, energy harvesters with compact structure, high power density, and long lifetime are highly desired. Since the first piezoelectric nanogenerator (NG) was developed in 2006,[2] a series of great progresses have been made on energy scavenging at nanoscale with piezoelectric,[3–6] triboelectric,[7–9] and pyroelectric[10,11] NGs. Combined with electrical rectification and energy storage, some NGs with alternating current (AC) signals have been demonstrated to drive self-powered nanosystems.[12–14] Since such self-powered nanosystems will have wide applications in different areas and circumstances, such as wireless sensor networks,[15,16] electrochemical reaction,[17–19] and chemical sensors,[20,21] it is highly desirable to develop more types of generators based on vastly different mechanisms to meet the demands of different operating conditions. Taking the biomedical applications as an example, micro/nanofluidic systems have been widely utilized in biosensors,[22] biomedical diagnostics,[23] and DNA analysis,[24] where conventional NGs are less effective for energy harvesting from the flowing fluid.

Herein, we demonstrated a streaming potential/current-based microfluidic generator (MFG), for converting the hydroenergy of fluid into continuous electrical output. The streaming potential/current phenomenon has been reported for energy conversion[25–27] and detection of flow velocity and solution concentration.[28–30] Generally, there are two types of fluid channels for streaming potential/current generation. One is the micro/nanochannel without inner structure; while, the other is the macroscopical channel with porous structure. Compared to porous channel, the empty micro/nanochannel has quite little power output because of its small contact area between liquid and solid. Thus, to enhance its output, we proposed an MFG with a new channel filled with quasi-porous patterns for larger power generation. Different from conventional porous materials, the shape and dimension of the patterns can be precisely designed and fabricated, which benefit the quantification of MFG. The MFG has a constant current output, which is independent of its external load. It can provide a continuous current output of ≈1.75 nA, when the potassium chloride (KCl) solution with a concentration of ≈1 μM flows through the device with a flow rate of 0.4 mL min^{-1}. Furthermore, we creatively demonstrated a self-powered fluid-sensor system by utilizing the MFG to power a single-nanowire (NW)-based pH sensor. Through integration of the MFG and nanosensor into a conventional micro/nanofluidic system, a self-powered lab-on-chip system can be potentially achieved, which should inspire the research area in biology, medicine, and analytical chemistry. As for the MFG, we demonstrated in this paper for the self-powered system, there are three key advantages in the design. Firstly, the soft lithography technology employed to fabricate the quasi-porous flow channel for the MFG helps to realize the easy and precise fabrication and replication of the device in large quantity. Secondly, every part in the device remains stationary during the electricity generation process so that the MFG has small size, simple structure, and high reliability. Moreover, different from conventional strain-based generators, the proposed MFG supplies a continuous direct current (DC) output. Therefore, it can directly drive other devices with no need of electrical rectifier and energy storage units, which could significantly reduce the size, cost, and energy loss of self-powered systems. Thus, our MFG is an outstanding example of self-powered nanotechnology for applications in biological sciences, environmental monitoring, defense technology, and even personal electronics.

The MFG consists of two chief components, a microfluidic chip and a pair of electrodes. The microfluidic chip with a micro channel is the most important part, determining the performance of the MFG. To increase the contact area between the liquid solution and the channel walls, a patterned micropillar array was designed in the channel to form a quasi-porous structure, as shown in **Figure 1**. Soft lithography technology[31] was employed to fabricate the microchannel, which is shown in Figure 1A. Firstly, an Si mold with desired patterns was fabricated and silanized before utilization. The silanization of Si prevents the adhesion with PDMS. Then, the PDMS prepolymer was casted onto the mold and got thermally cured under heating. In this manner, the patterned microchannel on the mold was printed onto the PDMS replica. Then, the PDMS replica was peeled off from the mold and tailored into the size of 20 mm in width and 35 mm in length. The channel locates in the center of the PDMS replica surface, and it has a shape of quasi-strip with its two ends

Dr. R. Zhang, Dr. S. Wang, Dr. M.-H. Yeh, Dr. L. Lin, R. Yu, Dr. L. Zheng, Prof. Z. L. Wang
School of Materials Science and Engineering
Georgia Institute of Technology
Atlanta, GA 30332-0245, USA
E-mail: zlwang@gatech.edu
Dr. R. Zhang, Prof. Z. Jiao
School of Automation Science and Electrical Engineering
Beihang University
Beijing 100191, China
Dr. C. Pan, Dr. Y. Zhang, Prof. Z. L. Wang
Beijing Institute of Nanoenergy and Nanosystems
Chinese Academy of Sciences
Beijing 100083, China

DOI: 10.1002/adma.201502477

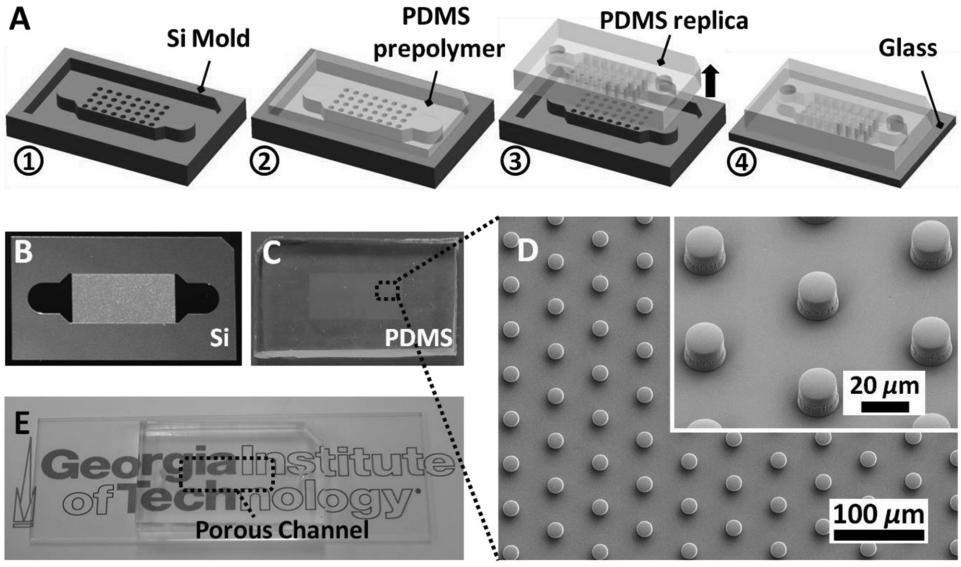

Figure 1. Fabrication and characterization of the microfluidic chip in MFG: A) fabrication of the microfluidic chip with soft lithography technology; B) photo of the Si mold with designed structure; C) photo of the patterned PDMS replica; D) SEM images of the micropillar arrays on PDMS replica. The inset shows a 30° tilted image with high magnification; and E) photo of the transparent microfluidic chip.

a little narrower than the middle. The micropattern covers the entire middle region of the channel, forming a quasi-porous structure. Two holes were punched at the two ends of the microchannel as the inlet and outlet. Finally, the PDMS replica was bonded onto a glass slide via oxygen plasma treatment. The as-fabricated Si mold and PDMS replica are shown in Figure 1B and 1C, respectively. Figure 1D shows a scanning electron microscopy (SEM) image of the micropattern in the channel. The micropillar array is uniform and regular across a large area, with the pillar's diameter of ≈18 μm and an interval of 50 μm. The entire microfluidic chip is transparent, with its photo given in Figure 1E. Such soft-lithography method is very economic, repeatable, and stable, and thus hundreds of PDMS replica can be produced using only one Si mold following the above process.[31]

The fabrication of this MFG was finished by mounting electrodes into the punched holes on the chip. As depicted in **Figure 2**A, two tubular electrodes were plunged into the holes. The tubular electrodes not only serve as conductor for charge collection, but also as the fluid inlet and outlet of the microchannel. In this research, the working fluid mainly used was 1 μM KCl aqueous solution (but not limited to). Driven by a syringe pump, the KCl solution runs through the MFG from the inlet to the outlet, via the porous structure in between. As shown in Figure 2B, once the KCl solution contacts the porous structure and inner walls of the PDMS replica, their interface on PDMS gets negatively charged via contact electrification. To keep the overall charge neutrality at interface between the PDMS surface and KCl solution, the negatively charged PDMS walls will attract cations, namely K^+ in this work, but exclude anions (Cl^-) in the solution, and the electrical double layer (EDL) is formed. In such a region, the charge neutrality of the solution is violated due to the presence of the EDL. When the solution flows under pressure, the transportation of K^+ ions in EDL along with the flow gives lead to a net positive charge transport, known as the streaming current (I_{str}). Meanwhile, the induced electric field created by the resulting polarization of charge distribution along the flowing axis leads to a streaming potential (V_{str}).[28,32] As illustrated in the bottom of Figure 2B, V_{str} increases with the larger flow displacement. Thus, there is a potential difference between the two electrodes of MFG. The potential difference drives electrons in the external circuit to move unidirectionally and continuously, which leads to the DC conduction current (I_{con}) of this MFG.

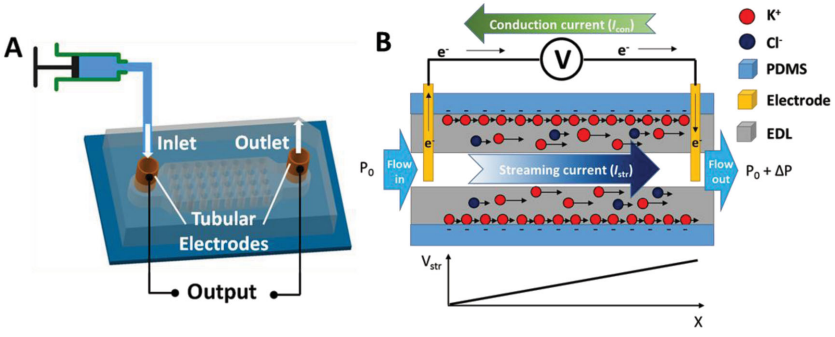

Figure 2. Schematics of the MFG: A) schematic of experiment apparatus and B) operating principle of the MFG.

The electrical output performances of the MFG were investigated experimentally. As shown in **Figure 3**A, when the syringe pump was turned on, a constant open-circuit voltage output of the proposed MFG was measured, which is ≈0.16 V at a flow rate of 0.4 mL min^{-1}. When the pump was turned off, the voltage output gradually decayed to disappear. Figure 3B shows that the corresponding short-circuit current output of this device is ≈1.75 nA under the same operating conditions as in Figure 3A. Also, both

Adv. Mater. **2015**,
DOI: 10.1002/adma.201502477

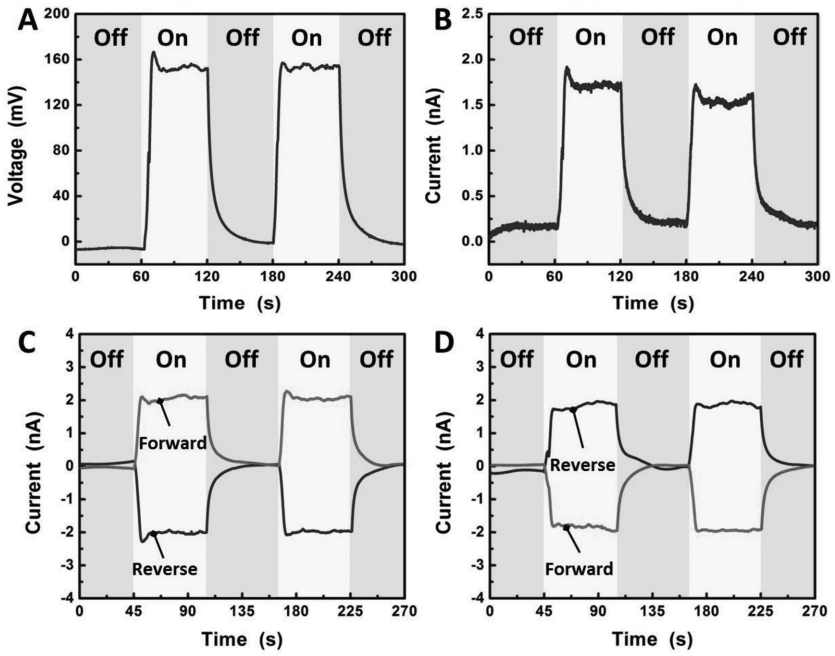

Figure 3. Electrical characteristics of the MFG: A) open-circuit voltage output; B) short-circuit current output; C) forward and reverse current outputs when flow direction is forward; and D) forward and reverse current outputs when flow direction is reversed.

the voltage and current outputs are steady during different on–off cycles. To verify that the electrical outputs are generated by the MFG rather than the measurement system, the switching-polarity test was carried out.[33] As shown in Figure 3C, a positive current output was observed when the outlet electrode of the MFG was connected to the positive probe of the ammeter (which is defined as forward connection), while the output was negative under the reversed connection. Meanwhile, when the fluid's flow direction was reversed, the opposite results were acquired as shown in Figure 3D. All of the above results confirm that the electricity was generated by the proposed MFG. To validate the performance of the MFG, a stability test was carried out for 7 d. As shown in Figure S1 (Supporting Information), no apparent performance degradation was observed during this period, which verified the good durability of the MFG.

Depending on the ion movement in the solution, the MFG gives a constant current output at steady state. To validate this characteristic, the MFG was connected to an external load of adjustable resistance (R_x). With the circuit diagram in **Figure 4**A, the current and voltage outputs were simultaneously measured. During the experiment, R_x was increased from 0 to 8 MΩ with a step of 2 MΩ. As depicted in Figure 4B, the current output remained a constant value with the variation of resistance, which demonstrates the MFG's nature as a constant current power source. And the voltage output rose from 0 to 12 mV proportionally with the increase of the resistance, consistent with the Ohm's law. The dependence of the short-circuit current on the flow rate was also studied. The flow rate input of the MFG was firstly increased from 0 to $0.4\ \mathrm{mL\ min^{-1}}$ with a step of $0.1\ \mathrm{mL\ min^{-1}}$, and then decreased back to 0 with a step of $0.4\ \mathrm{mL\ min^{-1}}$. As illustrated in Figure 4C, when both of the flow direction and electrical connection are at forward direction, the current output is positive and changes in the same trend with the flow rate. The plot of the current output versus flow rate input in the inset of Figure 4C indicates that the dependence of the current on the flow rate is almost linear. When the flow direction was reversed (represented as negative flow rate), the opposite result was obtained in Figure 4D. This set of results also clearly indicates that the proposed MFG has the potential to be utilized as an active flow rate sensor, with no need of external power supply.

The performance dependence of the MFG was further investigated. **Figure 5**A depicts the ion effect on the current output of the MFG. Three kinds of solutions, including Li^+, Na^+, and K^+ ions respectively, were selected as the working fluid. However, there is no apparent difference among the device current outputs, which show the good solution compatibility of the MFG. The solution concentration is a key factor for the MFG output. As indicated in Figure 5B, with the increase of KCl concentration, the current output is approximately constant at first when the KCl concentration is low (<10 μM), and then dramatically drops at higher concentration. When the concentration is 10 μM, the output reaches a maximum value of ≈2.45 nA. The MFG with DI water as working fluid was also tested as in Figure S2 (Supporting Information). Electrical outputs were also observed because of the presence of H^+ in DI water. However, the results are poorer than that using KCl solution, due to the high ion mobility of H^+-induced power dissipation.[25] Figure 5C shows the size effect of the micropatterns. With the increase of the diameters of micropillars, the current outputs increase proportionally, resulting from the linear augment of the contact area between fluid and channel. Besides micropillars, different shapes of the patterns were also fabricated to discuss the structure effect, including microtriangular prism and microquadrangular prism. As shown in Figure 5D, the micropillars with a diameter of 6 μm result to a similar output as the microtriangular prism with an edge length of 8 μm, which is ≈1 nA. The reason is that both structures have similar contact area. Similarly, the micropillars with diameter of 18 μm lead to the similar output as the microquadrangular prism with an edge length of 18 μm, reaching ≈2.5 nA.

Compared with conventional micro/nanogenerators with pulse outputs, the MFG which can provide a continuous DC output is particularly suitable to be employed in a self-powered system. No need to be rectified and/or stored, the electricity generated by the MFG can drive electronics directly and continuously, so that the system's cost, size, and energy loss are reduced significantly. NW based sensors have high sensitivity, small size and low power consumption.[34–36] Utilizing the MFG to power a NW based sensor, we demonstrated a self-powered nanosensor system as in **Figure 6**A. A single ZnO NW-based pH sensor was driven by the MFG to detect the pH values of different solutions. The ZnO NW was bonded

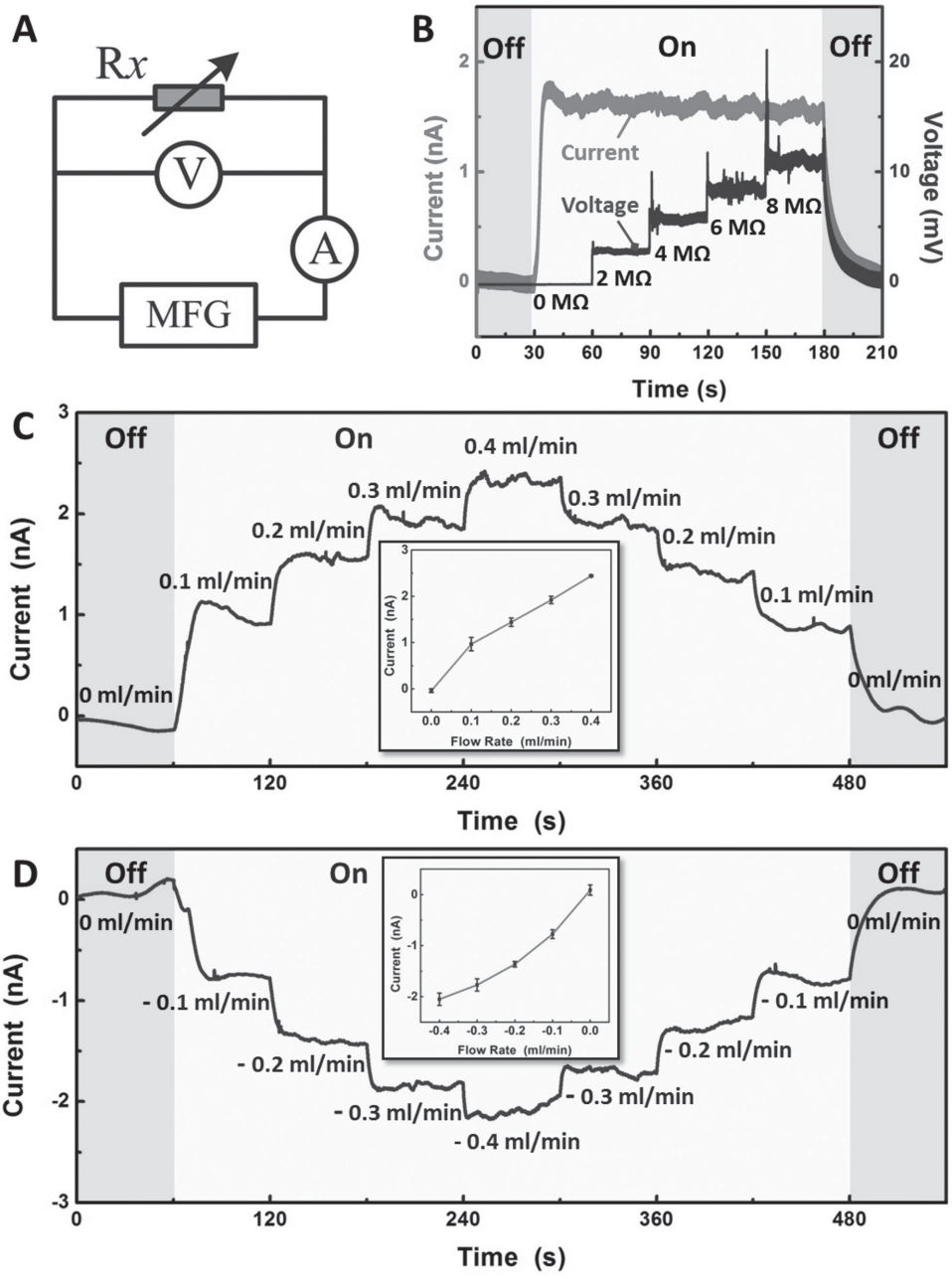

Figure 4. Determinants of the current output of the MFG: A) circuit diagram for voltage–current output measurements; B) voltage–current outputs of the MFG; C) short-circuit current output under forward flow direction. The inset shows forward-flow-rate versus current; and D) short-circuit current output under reverse flow direction. The inset shows the reverse-flow-rate versus current.

onto the substrate by sliver paste at its two ends, with epoxy totally covering the electrodes. The photo and optical microscopy image of this single-NW-based nanosensor are shown in the insets of Figure 6B. A voltmeter was utilized to detect the voltage across the nanosensor (as shown in Figure 6A). In this experiment, the nanosensor was put into different buffer solutions to detect their pH values. The change of pH results in a variation of the electrical conductivity of the ZnO NW. As stated above, since the MFG is a constant current source, the voltage across the NW will change under different pH values, which is in accordance with the result in Figure 4B. Figure 6B depicts the voltage across the NW based pH sensor. The voltage is about 22 mV when pH = 12. When the pH value is decreased to 5, the voltage output increases sharply to 65 mV. The result is repeatable and stable. After the systematical calibration, such MFG-driven self-powered pH-sensor system has a great potential to be incorporated into conventional micro/nanofluidic systems for real-time measurement and monitoring, which should inspire great research interests in biology, medicine and analytical chemistry.

In summary, we demonstrated a streaming potential/current based microfluidic DC generator, which has a patterned

Adv. Mater. 2015,
DOI: 10.1002/adma.201502477

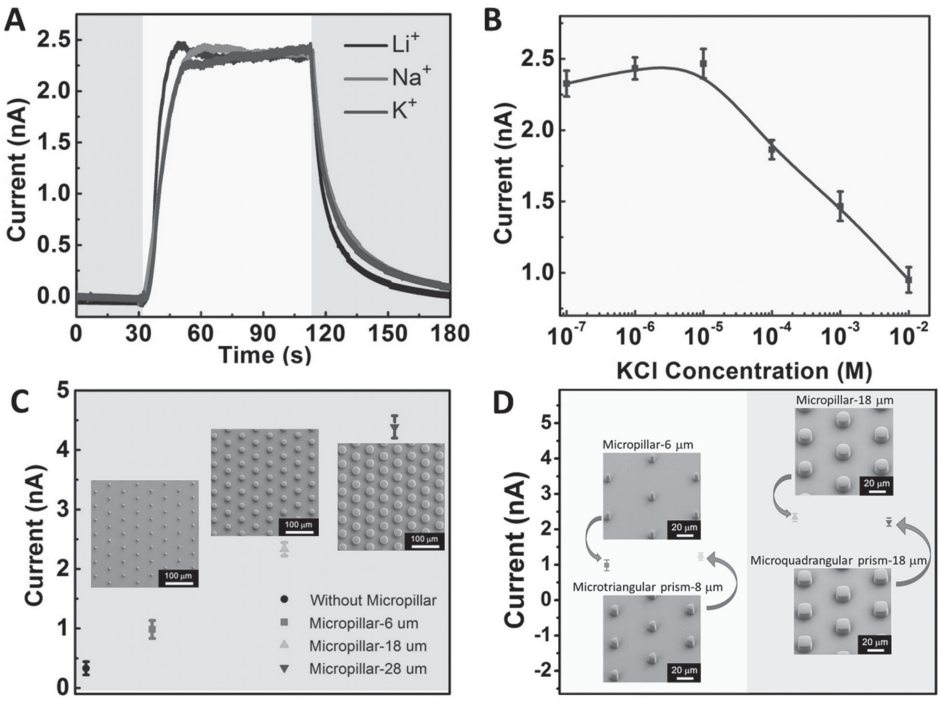

Figure 5. Performance dependence of the MFG: A) electrical characteristics of the MFG with different monovelent ion, i.e., Li^+, Na^+, and K^+ solutions. The concenretion of monovelent ion solutions were ≈1 μM and the flow rate was 0.1 mL min^{-1}; B) dependence of the short-circuit current on KCl concentration; C) short-circuit current output of MFG with different diameter of micorpillars, i.e., $D = 6$, 18, and 28 μm. MFG without micropattern, namely flat PDMS, was also performed as the reference; D) short-circuit current output of MFG with different structure of micropatterns, i.e., microtriangular prism (≈8 μm) and microquadrangular prism (≈18 μm). All of Data points are averaged under three independent tests, and the error bars indicate the average standard deviation for all points. The concentration of KCl solution was 1 μM and the flow rate was 0.1 mL min^{-1}.

micropillar array as the porous flow channel. The MFG converts mechanical energy from microfluid into continuous electrical output. With the magnitude of the current output not affected by external load, the MFG is a constant current source. It can provide a continuous current output of ≈1.75 nA for a KCl solution with a concentration of ≈1 μM and flow rate of 0.1 mL min^{-1}. Such microfluidic DC generators have the advantages of simple structure, long lifetime and low system cost. Moreover, it can be easily replicated using the soft lithography technology. For the purpose of building a self-powered system, the MFGs can be utilized to directly drive the continuous operation of electronic devices, due to its nature of the DC output. In this manner, a self-powered nanosensing system is demonstrated with the MFG as the power source for a single ZnO NW based pH sensor. By integrating the proposed MFG and nanosensor into the conventional micro/nanofluidic system, a self-powered lab-on-chip system can be expected, which should have wide applications in biology, medicine and analytical chemistry.

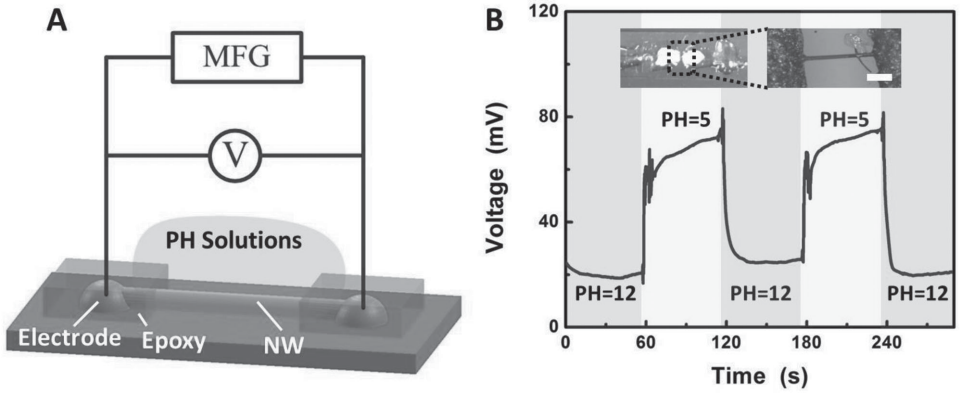

Figure 6. Schematic and test of the MFG based self-powered pH-sensor system: A) schematic of the self-powered nanosensing system; B) voltage output of the system. The insets show the single-NW-based pH sensor. Left: photo of the sensor. Right: optical microscopy image of the ZnO NW (length of the scale bar is 100 μm).

Supporting Information

Supporting Information is available from the Wiley Online Library or from the author.

Acknowledgements

R.Z., S.W., M.H.Y., and C.P. contributed equally to this work. This research was supported by US NSF, National Nature Science Foundation for Distinguished Young Scholars (No. 50825502), and the Thousands Talents Program and their innovation team. R.Z. is grateful for the fellowship from China Scholarship Council (CSC No. 2011602060). M.H.Y. thanks the support from Ministry of Science and Technology, Taiwan (MOST 103-2917-I-564-070).

Received: May 23, 2015
Revised: August 9, 2015
Published online:

[1] Z. L. Wang, *Adv. Mater.* **2012**, *24*, 280.
[2] Z. L. Wang, J. Song, *Science* **2006**, *312*, 242.
[3] X. Wang, J. Song, J. Liu, Z. L. Wang, *Science* **2007**, *316*, 102.
[4] Y. Qin, X. Wang, Z. L. Wang, *Nature* **2008**, *451*, 809.
[5] Y. Hu, Z. L. Wang, *Nano Energy* **2015**, *14*, 3.
[6] X. Wang, *Nano Energy.* **2012**, *1*, 13.
[7] F. R. Fan, Z. Q. Tian, Z. Lin Wang, *Nano Energy* **2012**, *1*, 328.
[8] G. Zhu, J. Chen, T. Zhang, Q. Jing, Z. L. Wang, *Nat. Commun.* **2014**, *5*, 3426.
[9] S. Wang, L. Lin, Z. L. Wang, *Nano Energy* **2015**, *11*, 436.
[10] Y. Yang, W. Guo, K. C. Pradel, G. Zhu, Y. Zhou, Y. Zhang, Y. Hu, L. Lin, Z. L. Wang, *Nano Lett.* **2012**, *12*, 2833.
[11] Y. Yang, J. H. Jung, B. K. Yun, F. Zhang, K. C. Pradel, W. Guo, Z. L. Wang, *Adv. Mater.* **2012**, *24*, 5357.
[12] Z. L. Wang, *Sci. Am.* **2008**, *298*, 82.
[13] Z. L. Wang, *Adv. Funct. Mater.* **2008**, *18*, 3553.
[14] Z. L. Wang, *ACS Nano* **2013**, *7*, 9533.
[15] S. Wang, L. Lin, Z. L. Wang, *Nano Lett.* **2012**, *12*, 6339.
[16] W. Tang, B. Meng, H. X. Zhang, *Nano Energy* **2013**, *2*, 1164.
[17] M. H. Yeh, L. Lin, P. K. Yang, Z. L. Wang, *ACS Nano.* **2015**, *9*, 4757.
[18] W. Tang, Y. Han, C. B. Han, C. Z. Gao, X. Cao, Z. L. Wang, *Adv. Mater.* **2015**, *27*, 272.
[19] G. Zhu, C. Pan, W. Guo, C. Y. Chen, Y. Zhou, R. Yu, Z. L. Wang, *Nano Lett.* **2012**, *12*, 4960.
[20] Z. H. Lin, G. Zhu, Y. S. Zhou, Y. Yang, P. Bai, J. Chen, Z. L. Wang, *Angew. Chem. Int. Ed.* **2013**, *52*, 5065.
[21] Z. Li, J. Chen, J. Yang, Y. Su, X. Fan, Y. Wu, C. Yu, Z. L. Wang, *Energy Environ. Sci.* **2015**, *8*, 887.
[22] N. V. Zaytseva, V. N. Goral, R. A. Montagna, A. J. Baeumner, *Lab chip* **2005**, *5*, 805.
[23] P. Yager, T. Edwards, E. Fu, K. Helton, K. Nelson, M. R. Tam, B. H. Weigl, *Nature* **2006**, *442*, 412.
[24] R. H. Liu, J. Yang, R. Lenigk, J. Bonanno, P. Grodzinski, *Anal. Chem.* **2004**, *76*, 1824.
[25] F. H. J. van der Heyden, D. J. Bonthuis, D. Stein, C. Meyer, C. Dekker, *Nano Lett.* **2006**, *6*, 2232.
[26] F. H. J. van der Heyden, D. J. Bonthuis, D. Stein, C. Meyer, C. Dekker, *Nano Lett.* **2007**, *7*, 1022.
[27] W. Olthuis, B. Schippers, J. Eijkel, A. van den Berg, *Sensors and Actuators B* **2005**, *111–112*, 385.
[28] F. H. J. van der Heyden, D. Stein, C. Dekker, *Phys. Rev. Lett.* **2005**, *95*, 116104.
[29] B. Bourlon, J. Wong, C. Miko, L. Forro, M. Bockrath, *Nat. Nanotechnol.* **2007**, *2*, 104.
[30] A. K. Newaz, D. A. Markov, D. Prasai, K. I. Bolotin, *Nano Lett.* **2012**, *12*, 2931.
[31] Y. Xia, G. M. Whitesides, *Angew. Chem. Int. Ed.* **1998**, *37*, 550.
[32] M. Z. Bazant, T. M. Squires, *Phys. Rev. Lett.* **2004**, *92*, 066101.
[33] X. Wang, J. Liu, J. Song, Z. L. Wang, *Nano Lett.* **2007**, *7*, 2475.
[34] Y. Cui, Q. Wei, H. Park, C. M. Lieber, *Science.* **2001**, *293*, 1289.
[35] A. Kolmakov, Y. Zhang, G. Cheng, M. Moskovits, *Adv. Mater.* **2003**, *15*, 997.
[36] P. Xie, Q. Xiong, Y. Fang, Q. Qing, C. M. Lieber, *Nat. Nanotechnol.* **2012**, *7*, 119.